Original Research

Multi-Parametric MRI Combined with Radiomics for the Evaluation of Lymphovascular Space Invasion in Cervical Cancer

Huanhuan Wang[1,†], Jie Meng[2,†], Guoqiang Dong[3,†], Lijing Zhu[4], Zhengyang Zhou[1,*],
Yuan Jiang[5,*], Li Zhu[2,*]

[1]Department of Radiology, Nanjing Drum Tower Hospital Clinical College of Nanjing University of Chinese Medicine, 210008 Nanjing, Jiangsu, China
[2]Departments of Radiology, Nanjing Drum Tower Hospital, Affiliated Hospital of Medical School, Nanjing University, 210008 Nanjing, Jiangsu, China
[3]Department of Interventional Radiology, The Second Affiliated Hospital of Bengbu Medical University, 233000 Bengbu, Anhui, China
[4]The Comprehensive Cancer Centre of Drum Tower Hospital, Affiliated Hospital of Medical School, Nanjing University, 210008 Nanjing, Jiangsu, China
[5]Departments of Gynaecology and Obstetrics, Nanjing Drum Tower Hospital, The Affiliated Hospital of Nanjing University Medical School, 210008 Nanjing, Jiangsu, China
*Correspondence: zyzhou@nju.edu.cn (Zhengyang Zhou); jsource80@163.com (Yuan Jiang); jullysaki@163.com (Li Zhu)
†These authors contributed equally.

Abstract

Background: To explore the feasibility of radiomic models using different magnetic resonance imaging (MRI) sequences combined with clinical information in evaluating the status of lymphovascular space invasion (LVSI) in cervical cancer. **Methods**: One hundred one cervical cancer patients were included from January 2018 to December 2020. All patients underwent 3.0T MRI examination including T2 weighted imaging (T2WI), diffusion weighted imaging (DWI) and contrast-enhanced T1 weighted imaging (T1WI + C) enhanced sequences. Age, preoperative squamous cell carcinoma (SCC) associated antigen value and the depth of muscular invasion were collected. The 101 patients were divided into training set and validation set. Three different models were developed using T2WI, DWI and T1WI + C parameters respectively. One model was developed combining the three different sequences. The diagnostic performance of each model was compared via receiver operating characteristic curve analysis. **Results**: Forty-eight cases were pathologically confirmed with lymphovascular space invasion. The average SCC value of the LVSI positive group (10.82 ± 20.11 ng/mL) was higher than that of the negative group (6.71 ± 14.45 ng/mL), however there was no significant statistical difference between the two groups. No clinical or traditional imaging features were selected by spearman correlation analysis. Among the corresponding radiomic models, the machine learning model based on multi-modality showed the best diagnostic efficiency in the evaluation of LVSI (receiver operating characteristic (ROC) curve of multimodal radiomics in the training set (area under the ROC curve (AUC) = 0.990 (0.975–0.999)) and in the validation set (AUC = 0.832 (0.693–0.971)). **Conclusions**: The diagnostic efficacy of radiomics is superior to conventional MRI parameters and clinical parameters. The radiomics-based machine learning model can help improve accuracy for the preoperative evaluation of LVSI in cervical cancer.

Keywords: cervical cancer; lymphovascular space invasion; machine learning; magnetic resonance imaging; radiomics

1. Introduction

Cervical cancer is the fourth leading cause of morbidity and mortality in women worldwide [1]. Several treatment strategies are available for cervical cancer including surgery, radiotherapy and concurrent chemoradiotherapy, depending on different clinical stages. Despite significant improvement in the development of diagnostic techniques, the long-term survival of patients with cervical cancer has not remarkably increased. Recent studies have reported that there are still overall 11%–22% and 28%–64% recurrence rate in IB–IIA and IIIB–IVA patients respectively [2–4]. This suggests that studies on prognostic factors of cervical cancer are of great importance.

Lymph node metastasis has been regarded as an independent prognostic factor in the progress of cervical cancer, while lymphovascular space invasion (LVSI) is a medium risk factor for the prognosis of cervical cancer. LVSI is a common pathological feature of malignant tumors; that is, tumor cells can be observed in the space surrounded by endothelial cells (including lymphatic space and vascular space) around the tumor tissue. Relevant studies have shown that LVSI is an independent risk factor of lymph node metastasis in cervical cancer [5,6]. In the process of tumor metastasis, tumor cells break off from the primary tumor entering into the vascular system and form tumor thrombi, which further spreads to invade other organs. Although the effect of LVSI on the prognosis of cervical cancer is still inconclusive, many studies have confirmed that positive LVSI indicates poor prognosis for cervical cancer [7–9]. The National Comprehensive Cancer Network (NCCN) clinical practice guidelines for cervical

cancer have also demonstrated that the treatment decision of early-stage cervical cancer varies on LVSI assessment. Stage IA1 patients with negative LVSI can be treated with simple hysterectomy, while those with positive LVSI require treatment similar to stage IA2 with modified radical hysterectomy with bilateral pelvic lymphadenectomy or sentinel lymph node visualization. Therefore, accurate assessment of LVSI is of great value for the formulation of individualized treatment plans for cervical cancer patients.

At present, the clinical evaluation of LVSI mainly depends on pathologic assessment. Accuracy of preoperative evaluation of LVSI is greatly restricted by the limited biopsy specimens. Therefore, it is extremely valuable to explore an accurate non-invasive method for preoperative evaluation of LVSI. Magnetic resonance imaging (MRI) has been widely used in the diagnosis and treatment of gynecological malignancies, including cervical cancer and endometrial cancer due to its excellent soft tissue resolution [10,11], as well as for the evaluation of LVSI [12]. Compared with traditional imaging, radiomics allows data mining into images through high-throughput extraction of quantitative features to support clinical decisions [13]. Some investigators have evaluated the role of radiomics in gynecological malignancies, including ovarian, cervical and endometrial cancer, mostly evaluating association with tumor prognostic factors, response to therapy and prediction of recurrence and metastasis. Other studies have correlated radiomic features with molecular/genomic profiling to classify prognosis [14,15].

The aim of this study was to establish radiomic models using three different MRI sequences (T2 weighted imaging (T2WI), diffusion weighted imaging (DWI), and contrast-enhanced T1 weighted imaging (T1WI + C)) combined with clinical information, in order to explore the application value of radiomic models in the preoperative evaluation of LVSI in cervical cancer.

2. Materials and Methods

2.1 General Data

This study retrospectively collected 157 patients who underwent gynecological pelvic MRI in our hospital from January 2018 to December 2020. Relevant clinical data including age, squamous cell carcinoma antigen (SCC) value (1–2 days before surgery) and postoperative pathological results were recorded.

The inclusion criteria for patients were as follows: ① patients underwent gynecological pelvic MRI examination before operation which included T2WI, DWI (b value was 800 s/mm^2) and contrast-enhanced T1WI sequence; ② patients were pathologically confirmed to have cervical cancer, and the interval between pathological examination and MRI examination was no more than 2 weeks.

The exclusion criteria for patients were as follows: ① any form of treatment before MRI examination, such as medication, surgery, radiotherapy and neoadjuvant chemotherapy; ② lesions too small to have been accurately identified on MRI; ③ poor quality MRI, such as images with significant artifacts; ④ incomplete imaging or clinical information.

As a result, 101 patients were included in this study and the patient enrollment process is shown in Fig. 1. We assigned 60% (n = 61) of the patients to the train set and 40% (n = 40) to the test set by stratified randomized sampling.

2.2 MRI Examination

All MRI examinations were performed on a 3.0T magnetic resonance scanner (Ingenia3.0T; Philips Healthcare, Best, the Netherlands). Magnetic resonance imaging sequences included the following: axial and sagittal T2-weighted turbo spin-echo (T2W-TSE) sequence; axial T1 high resolution isotropic volume examination (THRIVE) sequence; axial and sagittal T2 spectral presaturation attenuated inversion recovery (SPAIR). The contrast medium was Omniscan (GE Healthcare Ireland, Shanghai, China), which was injected intravenously at a rate of 3.0 mL/s with the dose of 0.2 mL/kg body weight, followed by 15 mL saline flush. The high pressure injector used was Medrad Spectris Solaris EP MR Injector System (One Medrad Drive, Indianola, PA, USA). B values of 0 and 800 s/mm^2 were used for DWI and apparent diffusion coefficient (ADC) maps were automatically generated and uploaded by post-processing software. The entire MRI scanning lasted approximately 15 min.

2.3 MRI Acquisition and Preprocessing

T2WI, DWI (b value = 800 s/mm^2) and T1WI + C sequences were used for analysis in this study. Two radiologists with experience in gynecological imaging read the images independently. Depth of myometrial invasion ($\geq$1/2 cervical interstitium/<1/2 cervical interstitium) were evaluated simultaneously. In the case of disagreement between the two radiologists, the lesion scope and depth of myometrial invasion were finally determined after joint discussion. The maximum diameter of the lesion on the crosssection and corresponding ADC value were recorded.

2.4 MRI Lesion Segmentation

MRI images of all patients (including axial T2WI, DWI and T1WI + C sequences) were imported into ITK-SNAP 3.0 software (Cognitica, Philadelphia, PA, USA; http://www.itksnap.org) in digital imaging and communications in medicine (DICOM) format. The identified lesions were manually segmented layer by layer by a radiologist with 4 years' experience in gynecological imaging and rechecked by a second radiologist with 15 years' experience. One week later, T2WI, DWI and T1WI + C images of 25 patients were randomly selected and outlined again for intraclass correlation coefficient (ICC) feature screening.
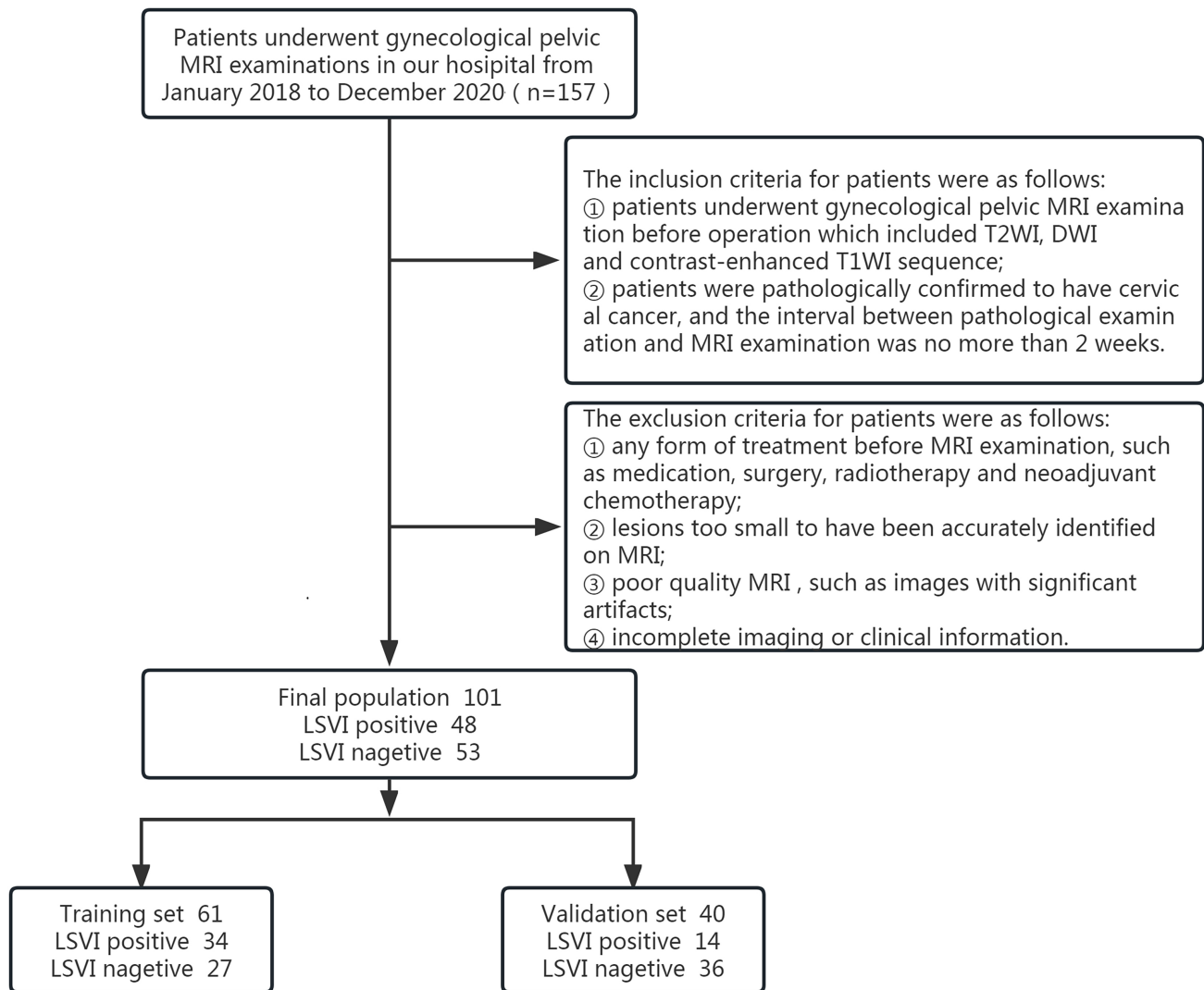
Fig. 1. Flowchart of inclusion. LVSI, lymphovascular space invasion; MRI, magnetic resonance imaging; T2WI, T2 weighted imaging; DWI, diffusion weighted imaging; T1WI, T1 weighted imaging.

The criteria for manual segmentation: (1) outline along the boundary of the lesion in order for the maximum volume of interest (VOI); (2) necrosis and bleeding area inside the lesion were included in order to reflect the heterogeneity of the tumor; (3) adjacent organs such as rectum and bladder were avoided.

2.5 Radiomics

The workflow of radiomics is shown in Fig. 2.

2.6 Feature Extraction

A total of 1158 features were extracted from T2WI, DWI and T1WI + C modes, including morphological features, first-order statistical features, and texture features (gray level co-occurrence matrix, GLCM; gray level run-length matrix, GLRLM; gray level region size matrix, GLSZM; gray level difference matrix, GLDM). Higher-order features were extracted after Laplacian Gaussian

transform and Wavelet transform. Radiomics features were extracted using IBSI-compliant pyradiomics software (version 3.0.1) (https://www.radiomics.io/). Image preprocessing was performed before feature extraction, including resampling to a voxel size of $1 \times 1 \times 1$, gray level discretization using binwidth of 5, and image normalization using z-score transformation. In order to evaluate the inter-observer agreement, 25 cases were randomly selected for segmentation and feature extraction. According to the 95% confidence interval estimated by intraclass correlation coefficient (ICC), it was classified as excellent (ICC = 0.90–1.00), good (ICC = 0.75–0.90), moderate (ICC = 0.50–0.75), or fair (ICC <0.50). ICC >0.75 was considered as good reproducibility, and features with ICC $\leq$0.75 were excluded.

2.7 Feature Selection

The 101 lesions were divided into the training set and the validation set according to time period. For the training set, features with high stability were first screened out
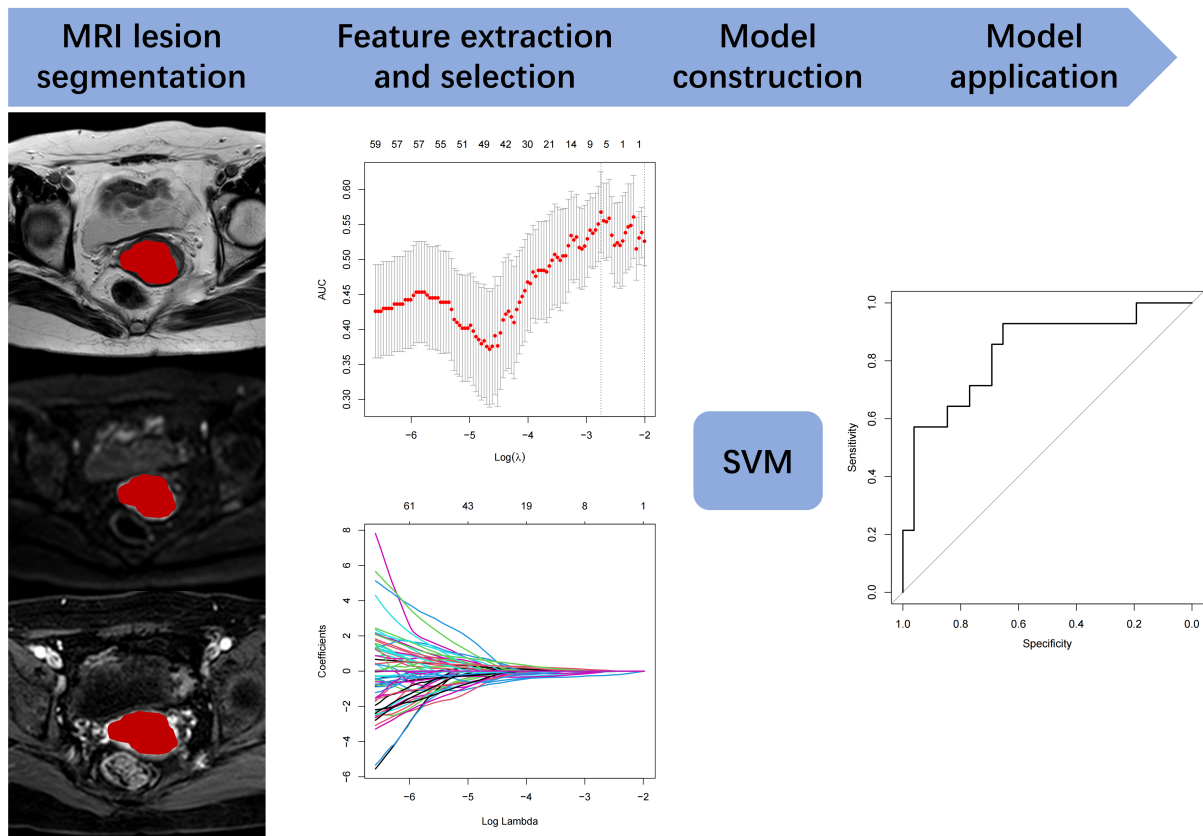
Fig. 2. Workflow of this research. MRI, magnetic resonance imaging; SVM, support vector machine; ROC, receiver operating characteristic; AUC, area under the ROC curve.

according to the intra-group and inter-group consistency of feature extraction (ICC >0.75), and were then selected using the least absolute shrinkage and selection operator (LASSO) logistic regression classifier. Furthermore, the penalty parameters were adjusted by $10\times$ cross validation, with features of non-zero coefficient being used as the correlation feature of cervical cancer lymphovascular space invasion (Fig. 3).

2.8 Radiomics Model Construction and Validation

Support vector machine (SVM) was used for the model establishment. SVM was implemented using the "e1071" package (https://CRAN.R-project.org/package=e1071) of R software (version 3.6.1, http://www.r-project.org). The type of SVM is "eps-regression", of which the kernel function is radial basis. The total number of support vectors is 225.

2.9 Statistical Analysis

All statistical analysis were performed using Rstudio (https://www.rstudio.com). Continuous quantitative data with a normal distribution were expressed as the mean $\pm$ standard deviation (SD). Categorical variables and continuous variables were compared by Chi-square test and Student t test respectively. Receiver operating characteristic (ROC) curve analysis and area under the ROC curve (AUC) were performed to detect the performances of the established models. The accuracy, sensitivity and specificity were calculated at the same time. A p value < 0.05 was considered statistically significant.

3. Results

3.1 Clinical Data

A total of 101 patients were included in this study (mean age: 53.42 ± 10.01 years, range: 29–76 years) (Table 1). All the cases were pathologically confirmed as cervical cancer with the International Federation of Gynecology and Obstetrics (FIGO) stage IA–IIIC (cervical squamous cell carcinoma 84, adenocarcinoma 16 and mixed adenoendocrine carcinoma 1). 48 cases were pathologically confirmed with lymphovascular space invasion with the remaining 53 with no lymphovascular space invasion. SCC values of the enrolled patients ranged from 0.46 to 100 ng/mL, with an average of 8.66 ± 17.40 ng/mL. The average SCC value of the LVSI positive group (10.82 ± 20.11 ng/mL) was higher than that of the LVSI negative group (6.71 ± 14.45 ng/mL), however there was no significant statistical difference between the two groups.
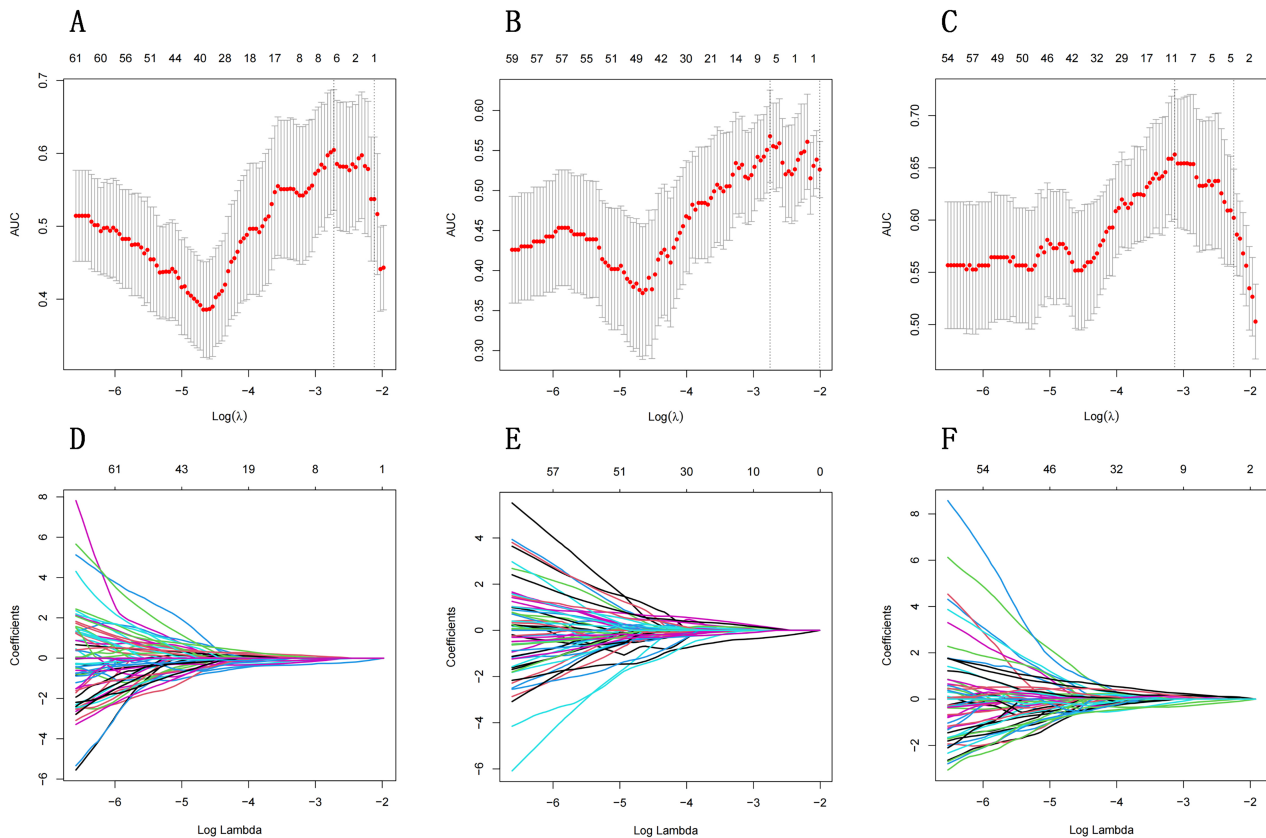
Fig. 3. Selection of radiomics features using least absolute shrinkage and selection operator (LASSO) regression. (A–C) show the optimal penalty coefficient λ (lambda) for DWI, contrast-enhanced T1 weighted imaging (TIWI + C), and T2WI modalities by adjusting different parameters using LASSO through 10-fold cross-validation, respectively. The minimum criterion and 1 standard error of the minimum criterion (1- standard error (SE) criterion) were used to draw vertical dashed lines at the optimal value. (D–F) respectively show the profile of the cable coefficients drawn according to the Log(λ) sequence. Each curve represents the coefficient change trajectory of a feature. The abscissa is the parameter, and the ordinate is the coefficient.

3.2 Results of Radiomics Feature Extraction, Selection and Model Construction

3.2.1 Feature Extraction

A total of 101 lesions were included in this study. Features of 1158 were extracted from the images of each mode, and 3474 features were extracted from the three modes.

3.2.2 Feature Selection

All features extracted from each mode were retained according to inter-observer ICC coefficients (greater than 0.75), and then assessed by using LASSO regression algorithm. Twenty-one features were kept for the model building (9 from T2WI, 6 from DWI, 6 from ADC) (Table 2). No clinical features or traditional imaging features were selected by spearman correlation analysis (Table 1).

3.2.3 Construction and Selection of Radiomics Model

SVM was used to establish a binary radiomics classifier to distinguish the lesion status of lymphovascular space invasion. The corresponding radiomic models were established based on different single modality and multi-modality (combined with T2WI, DWI and T1WI + C). Among them, the machine learning model based on multi-modality showed the best diagnostic efficiency in the evaluation of LVSI with AUC of 0.990 in the training set (sensitivity of 0.912 and specificity of 1.000) and AUC of 0.832 in the validation set (sensitivity of 0.929 and specificity of 0.654) (Figs. 4,5,6).

4. Discussion

Due to excellent soft tissue resolution, multi-parameter and multi-sequence imaging, MRI plays an important role in the clinical practice for cervical cancer. In recent years, the rise of radiomics has further expanded the application of MRI, enabling clinicians to deeply explore the hidden information in images [15]. The aim of this study was to construct radiomic models by using three conventional sequences (T2WI, DWI and T1WI + C) and to explore the new application of conventional sequences in the preoperative evaluation of LVSI in cervical cancer.

Table 1. General information of the patients.

	Total	LVSI (+)	LVSI (−)	p
	(n = 101)	(n = 48)	(n = 53)	
Age (years)	53.42 ± 10.01	53.25 ± 9.72	53.57 ±10.36	0.853
SCC (ng/mL)	8.66 ± 17.40	10.82 ± 20.11	6.71 ± 14.45	0.133
Depth of myometrial invasion				0.336
≥1/2 Cervical interstitium	80	40	40	
<1/2 Cervical interstitium	21	8	13	
Maximum diameter (cm)	3.41 ± 1.19	3.34 ± 1.14	3.47 ± 1.24	0.651
ADC value (10^{-6} mm^2/s)	797.58 ± 174.16	774.46 ± 141.56	818.52 ± 198.19	0.349
Pathology n (%)				
Squamous carcinoma	84 (83.17)	35 (34.65)	49 (48.51)	
Adenocarcinoma	16 (15.84)	12 (11.88)	4 (3.96)	
Mixed adenoendocrine carcinoma	1 (0.99)	1 (0.99)	0 (0)	

Note: Age, SCC, maximum diameter of tumor, and ADC value are presented as mean ± standard deviation.

LVSI, lymphovascular space invasion; SCC, squamous cell carcinoma; ADC, apparent diffusion coefficient.
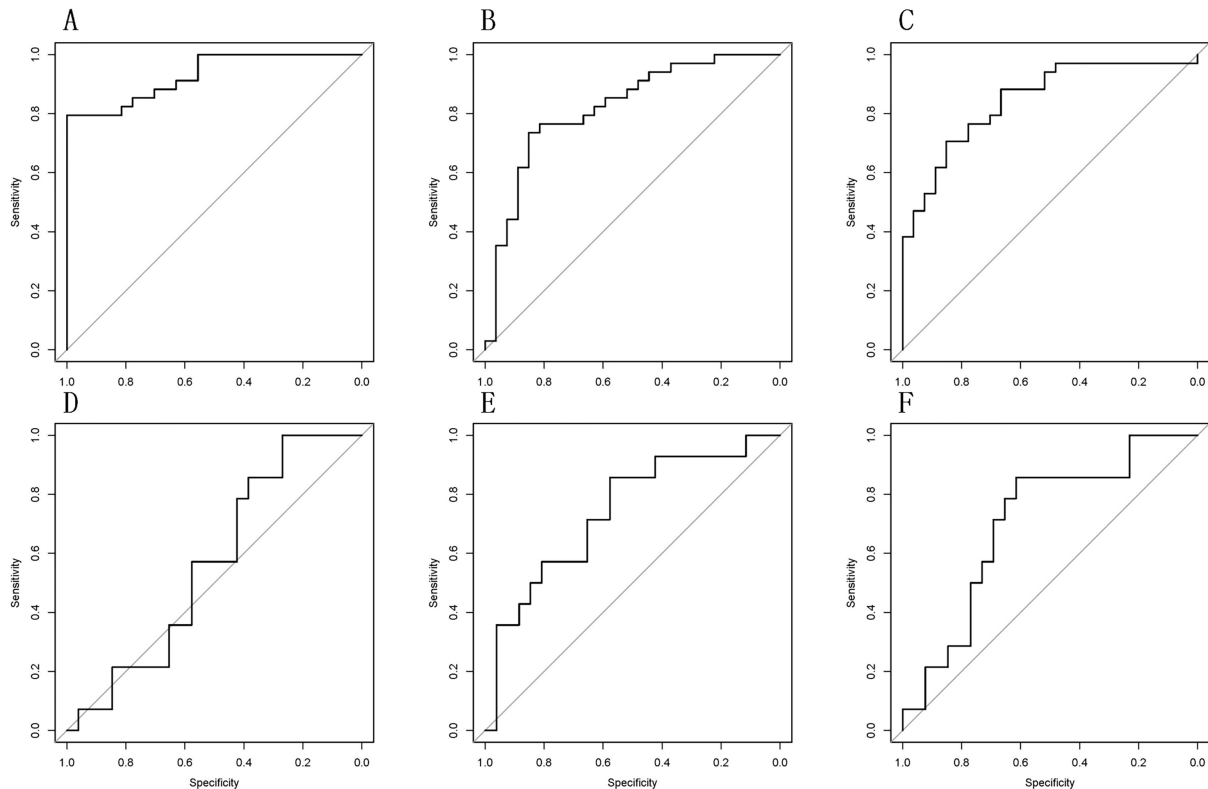

Fig. 4. Receiver operating characteristic (ROC) curve for preoperative evaluation of lymphovascular space invasion in cervical cancer based on single-modality radiomics. (A–C) ROC curves of T2WI, DWI and T1WI + C modes in the training set (area under the ROC curve (AUC) values are 0.929, 0.845 and 0.819, respectively). (D–F) ROC curves of T2WI, DWI and T1WI + C modes in the validation set ROC curve (AUC values are 0.563, 0.703, 0.739, respectively).

4.1 Clinical Parameters in Evaluating LVSI of Cervical Cancer

Clinical parameters including age, preoperative SCC value and the depth of muscular invasion were collected for this study, with no significant difference being found between the LVSI positive and negative group.

SCC is a serine protease inhibitor, which inhibits cell apoptosis and participates in the metabolism, proliferation, as well as differentiation of tumor cells. The average SCC value of patients enrolled in this study was 8.66 ± 17.40 ng/mL, which was similar to Li *et al.* [16] result (9.7 ± 16.9 ng/mL) in patients with cervical cancer prior to treat-

Table 2. Radiomics features of different MR modalities for differentiating lymphovascular space invasion in cervical cancer.

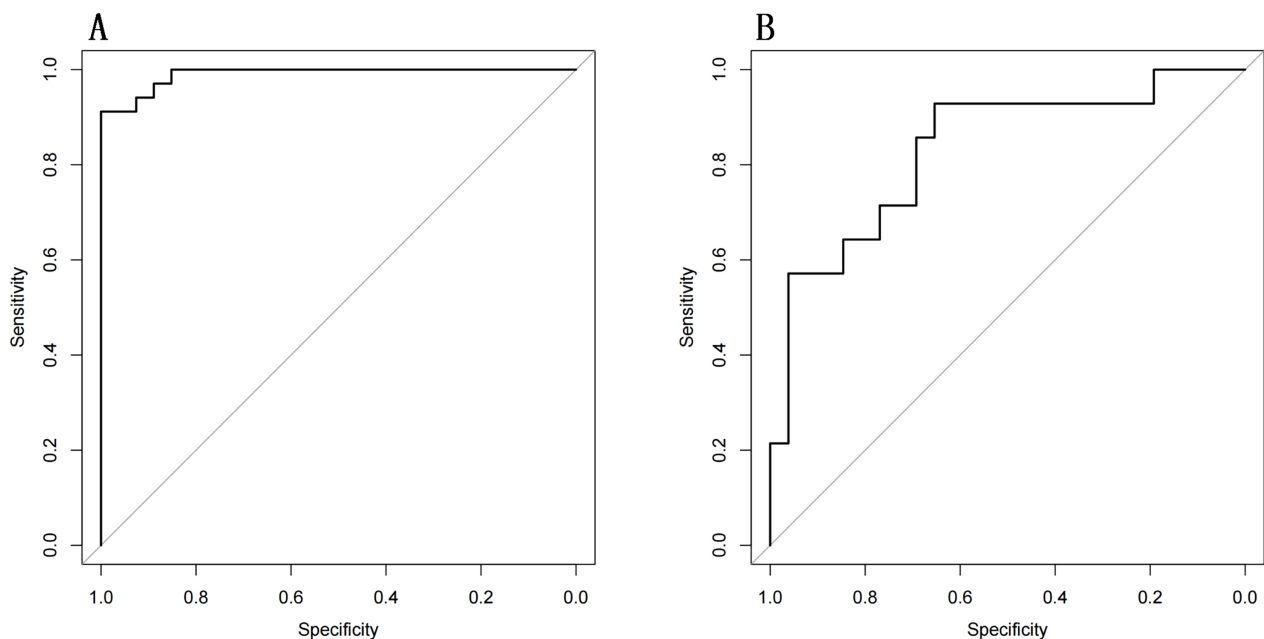| Model	Feature	Coefficient
T2	T2_wavelet.LHL_gldm_LargeDependenceLowGrayLevelEmphasis	−0.0150103717082837
	T2_wavelet.LHH_glcm_MCC	−0.333102279446099
	T2_wavelet.LHH_glszm_GrayLevelNonUniformityNormalized	−0.139919403617482
	T2_wavelet.LHH_glszm_SmallAreaEmphasis	0.0366815585921708
	T2_wavelet.LHH_glszm_SmallAreaLowGrayLevelEmphasis	0.263604565314742
	T2_wavelet.HLH_glszm_GrayLevelNonUniformityNormalized	0.115882962627615
	T2_wavelet.HLH_glszm_LowGrayLevelZoneEmphasis	0.170168865479784
	T2_wavelet.HLH_glszm_SmallAreaEmphasis	−0.239807378370699
	T2_wavelet.HHH_glszm_SmallAreaLowGrayLevelEmphasis	0.156686251059209
DWI	DWI_log.sigma.4.0.mm.3D_glszm_SmallAreaLowGrayLevelEmphasis	−0.0388555271048709
	DWI_wavelet.HLH_glszm_SmallAreaLowGrayLevelEmphasis	−0.0647164659164984
	DWI_wavelet.HHL_glcm_Imc2	−0.255252033880791
	DWI_wavelet.HHL_glcm_MCC	−0.0247464157443933
	DWI_wavelet.HHH_glcm_MCC	−0.0245653313656513
	DWI_wavelet.HHH_glszm_GrayLevelNonUniformityNormalized	0.0571260101709459
T1 + C	T1C_wavelet.HLH_firstorder_Skewness	0.127804041567352
	T1C_wavelet.HLH_glcm_Imc2	−0.300103234601108
	T1C_wavelet.HHL_firstorder_Median	0.0819543795798403
	T1C_wavelet.HHL_firstorder_Skewness	−0.0181913948467193
	T1C_wavelet.HHH_glszm_SizeZoneNonUniformityNormalized	0.0943811086627695
	T1C_wavelet.LLL_gldm_LargeDependenceLowGrayLevelEmphasis	−0.0271204202363728

Fig. 5. ROC curve of multimodal radiomics model for preoperative evaluation of lymphovascular space invasion in cervical cancer. (A) ROC curve of multimodal radiomics in the training set (AUC = 0.990 [95% confidence interval (95% CI): 0.975–0.999] with sensitivity of 0.912 and specificity of 1.000). (B) ROC curve of multimodal radiomics in the validation set (AUC = 0.832 [95% CI: 0.693–0.971] with sensitivity of 0.929 and specificity of 0.654).

ment. Our study demonstrated that the mean value of SCC in the LVSI positive group (10.82 ± 20.11 ng/mL) was higher than that in the LVSI negative group (6.71 ± 14.45 ng/mL), but no significant difference was found between the two groups ($p = 0.133$). The study of Yuan *et al*. [17] also suggested similar results, with no significant correlation between SCC level and LVSI. However, a different conclusion was reported as positive SCC being significantly
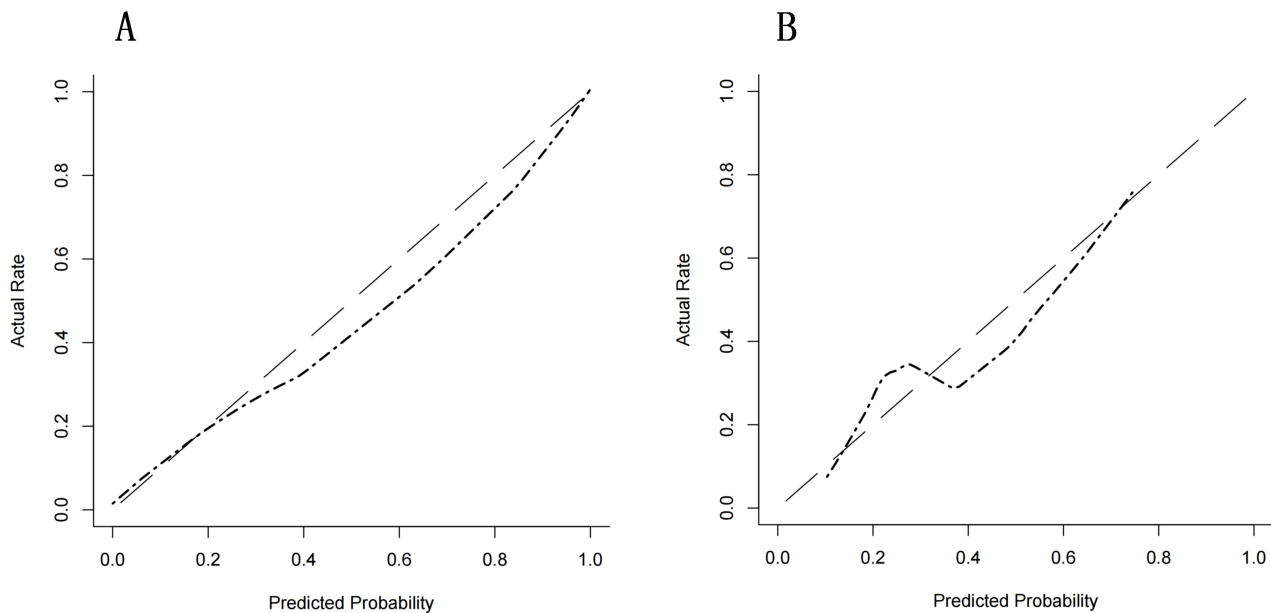
Fig. 6. Calibration curve of prediction model for multimodal radiomics alignment. (A) Calibration curve of multimodal radiomics in the training set (Sig = 0.999). (B) Calibration curve of multimodal radiomics in validation dataset (Sig = 0.461).

correlated with LVSI, which may be because the qualitative method used was different from the quantitative analysis method in this study [18]. Therefore, the assessment value of SCC level in evaluating LVSI of cervical cancer needs to be further explored in a larger sample size.

4.2 Conventional Imaging Parameters in Evaluating LVSI of Cervical Cancer

The maximum diameter and ADC value of the tumor were measured in this study, with no significant difference being confirmed between the two groups ($p = 0.651$ and 0.349 respectively). Malek *et al*. [19] showed that the mean ADC value of the LVSI positive group ($0.83 \pm 0.17 \times 10^{-3}$ mm^2/s) was lower than that of LVSI negative group ($1.05 \pm 0.25 \times 10^{-3}$ mm^2/s), which was similar with our results (Table 1). LVSI is an indicator of tumor invasiveness. A tumor with high invasiveness tends to grow faster with higher cell density and less extracellular space, leading to limited diffusion of water molecules, resulting in a decreased ADC value [20,21]. Their study also showed significant differences in ADC values between the two groups, suggesting that ADC values can reflect the LVSI status of cervical cancer. However, our study did not find a significant statistical difference between the two groups, suggesting that future studies are needed for validation.

4.3 Radiomics Model in Evaluating LVSI of Cervical Cancer

Compared with the clinical and traditional imaging parameters used in this study, radiomics parameters showed great potential in the preoperative LVSI evaluation of cervical cancer (Figs. 4,5). T2_wavelet.LHH_glcm_MC,

T2_wavelet.LHH_glszm_SmallAreaLowGrayLevelEmphasis, DWI_wavelet.HHL_glcm_Imc2 and T1C_wavelet. HLH_glcm_Imc2 showed higher weights during the selection of features. GLCM contains spatial information about the relationship of pixel pairs with similar or specific intensity within an image, while GLSZM measures groups of pixels with the same intensity regard-less of direction. Both of them can reflect the heterogeneity of the tumor. Peeken *et al*.'s [22] research showed similar results as the wavelet features could reflect multifrequency information of spatial heterogeneity of tumors. Among the features, wavelet.HLH_glcm_Imc2 were negatively correlated with LVSI in DWI and T1WI models, indicating lower wavelet.HLH_glcm_Imc2 and less linear structures in lesions with LVSI [23].

Numerous studies have applied radiomics in the evaluation of LVSI in cervical cancer. For example, Wu *et al*. [24] showed that radiomics features of T2WI, T2 with fat suppression (T2-FS), DWI and dynamic contrast enhanced (DCE) sequences can help in evaluating LVSI of cervical cancer with AUC values ranging from 0.659 to 0.814, among which, DCE sequence showed the best performance. Similar results were produced in our study, as AUC values of the single-modality radiomics parameters ranged from 0.845 to 0.929 in the training set and 0.563 to 0.739 in the validation set, of which the T1WI + C sequence showed the best performance. Similar findings may suggest that radiomics features related to tumor perfusion are better at evaluating LVSI than the diffusion-related radiomics features. Although the assessment efficiency of DCE sequence used by Wu *et al*. [24] is slightly superior to that of T1WI + C sequence used in this study, it requires a more rigor-

ous operation and longer scanning time than T1WI + C sequence. Therefore, the routine sequence (T1WI + C) was eventually chosen in this study.

In addition, our study further established the radiomics model combined three different modality parameters, including T2WI, DWI and T1WI + C. The results demonstrated that performance of the comprehensive model in evaluating LVSI was significantly better than that of the single-mode radiomics model, with an AUC value of 0.990 in the training set and 0.832 in the validation set (Figs. 5,6). The research of Huang *et al.* [25] also showed similar results, with their AUC values of single-mode radiomics model ranged from 0.681 to 0.878, while AUC value of the comprehensive model was 0.922. This suggests that with more parameters involved, more accurate information of tumor internal characteristics can be provided, resulting in better prediction efficiency.

This study has some limitations. First, the results were established in a single center with limited sample size, and this study did not review external validation datasets. Future studies should recruit a larger cohort of patients in multi-center study to confirm our results. Second, manual segmentation of the region of interest (ROI) is a time-consuming process and more subjective, automatic segmentation is crucial and objective for promoting the feasibility of radiometric measures. Third, because of limited cases and subtypes, we did not compare the depth of myometrial invasion subgroups. Nevertheless, our results suggest that the benefits of a radiomics model to suspect the presence of LVSI of cervical cancer.

5. Conclusions

Radiomics holds great potential in the evaluation of LVSI in cervical cancer. Its diagnostic efficacy is superior to conventional MRI and clinical parameters. Radiomics has the potential to be an effective method for preoperative LVSI assessment for cervical cancer, and can provide strong support for clinical diagnosis and treatment protocols.

Availability of Data and Materials

The datasets used and analyzed during the current study are available from the corresponding author on reasonable request.

Author Contributions

LiZ, YJ and ZZ designed the research study. YJ performed the research. LijingZ collected data and made treatment decision. HW, JM and GD analyzed the data and wrote the manuscript. All authors contributed to editorial changes in the manuscript. All authors read and approved the final manuscript. All authors have participated sufficiently in the work and agreed to be accountable for all aspects of the work.

References

[1] Sung H, Ferlay J, Siegel RL, Laversanne M, Soerjomataram I, Jemal A, *et al.* Global Cancer Statistics 2020: GLOBOCAN Estimates of Incidence and Mortality Worldwide for 36 Cancers in 185 Countries. CA: A Cancer Journal for Clinicians. 2021; 71: 209–249.

[2] Peiretti M, Zapardiel I, Zanagnolo V, Landoni F, Morrow CP, Maggioni A. Management of recurrent cervical cancer: a review of the literature. Surgical Oncology. 2012; 21: e59–66.

[3] Cohen PA, Jhingran A, Oaknin A, Denny L. Cervical cancer. Lancet (London, England). 2019; 393: 169–182.

[4] Quinn MA, Benedet JL, Odicino F, Maisonneuve P, Beller U, Creasman WT, *et al.* Carcinoma of the cervix uteri. International Journal of Gynaecology and Obstetrics: the Official Organ of the International Federation of Gynaecology and Obstetrics. 2006; 95: S43–S103.

[5] Yu F, Chen Y, Huang L, Nie G. Risk factors of node metastasis in cervical carcinoma. European Journal of Gynaecological Oncology. 2016; 37: 662–665.

[6] Liu Y, Zhao LJ, Li MZ, Li MX, Wang JL, Wei LH. The Number of Positive Pelvic Lymph Nodes and Multiple Groups of Pelvic Lymph Node Metastasis Influence Prognosis in Stage IA-IIB Cervical Squamous Cell Carcinoma. Chinese Medical Journal. 2015; 128: 2084–2089.

[7] Yamauchi M, Fukuda T, Wada T, Kawanishi M, Imai K, Hashiguchi Y, *et al.* Comparison of outcomes between squamous cell carcinoma and adenocarcinoma in patients with surgically treated stage I-II cervical cancer. Molecular and Clinical Oncology. 2014; 2: 518–524.

[8] Margolis B, Cagle-Colon K, Chen L, Tergas AI, Boyd L, Wright JD. Prognostic significance of lymphovascular space invasion for stage IA1 and IA2 cervical cancer. International Journal of Gynecological Cancer: Official Journal of the International Gynecological Cancer Society. 2020; 30: 735–743.

[9] Erdem B, Çelebi İ, Aşıcıoğlu O, Akgöl S, Yüksel İT, Özaydin İY, *et al.* Preoperative prediction of retroperitoneal lymph node involvement in clinical stage IB and IIA cervical cancer. Journal of Cancer Research and Therapeutics. 2022; 18: 1548–1552.

[10] Zhou Y, Gu HL, Zhang XL, Tian ZF, Xu XQ, Tang WW. Mul-

tiparametric magnetic resonance imaging-derived radiomics for the prediction of disease-free survival in early-stage squamous cervical cancer. European Radiology. 2022; 32: 2540–2551.

[11] Fu JX, Cui YH, Xu LQ, Shen P, Liu XL, Chen CL, *et al*. Preoperative Evaluation of 3D-MRI on the Depth of Myometrial Invasion of Endometrial Carcinoma: 3D Study of Endometrial Carcinoma. Clinical and Experimental Obstetrics & Gynecology. 2022; 49: 222.

[12] Yang W, Qiang JW, Tian HP, Chen B, Wang AJ, Zhao JG. Minimum apparent diffusion coefficient for predicting lymphovascular invasion in invasive cervical cancer. Journal of Magnetic Resonance Imaging: JMRI. 2017; 45: 1771–1779.

[13] Lambin P, Rios-Velazquez E, Leijenaar R, Carvalho S, van Stiphout RGPM, Granton P, *et al*. Radiomics: extracting more information from medical images using advanced feature analysis. European Journal of Cancer (Oxford, England: 1990). 2012; 48: 441–446.

[14] Manganaro L, Nicolino GM, Dolciami M, Martorana F, Stathis A, Colombo I, *et al*. Radiomics in cervical and endometrial cancer. The British Journal of Radiology. 2021; 94: 20201314.

[15] Bogani G, Chiappa V, Lopez S, Salvatore C, Interlenghi M, D'Oria O, *et al*. Radiomics and Molecular Classification in Endometrial Cancer (The ROME Study): A Step Forward to a Simplified Precision Medicine. Healthcare (Basel, Switzerland). 2022; 10: 2464.

[16] Li T, Huang H, Hu Y, Chen H, Li R, Lu H, *et al*. Rs2686344 and serum squamous cell carcinoma antigen could predict clinical efficacy of neoadjuvant chemotherapy for cervical cancer. Current Problems in Cancer. 2021; 45: 100755.

[17] Yuan CC, Wang PH, Ng HT, Tsai LC, Juang CM, Chiu LM. Both TPA and SCC-Ag levels are prognostic even in high-risk stage Ib-IIa cervical carcinoma as determined by a stratification analysis. European Journal of Gynaecological Oncology. 2002; 23: 17–20.

[18] Yang H, Hu H, Gou Y, Hu Y, Li H, Zhao H, *et al*. Combined detection of Twist1, Snail1 and squamous cell carcinoma antigen for the prognostic evaluation of invasion and metastasis in cervical squamous cell carcinoma. International Journal of Clinical Oncology. 2018; 23: 321–328.

[19] Malek M, Rahmani M, Pourashraf M, Amanpour-Gharaei B, Zamani N, Farsi M, *et al*. Prediction of lymphovascular space invasion in cervical carcinoma using diffusion kurtosis imaging. Cancer Treatment and Research Communications. 2022; 31: 100559.

[20] Rosenkrantz AB, Padhani AR, Chenevert TL, Koh DM, De Keyzer F, Taouli B, *et al*. Body diffusion kurtosis imaging: Basic principles, applications, and considerations for clinical practice. Journal of Magnetic Resonance Imaging: JMRI. 2015; 42: 1190–1202.

[21] Yue W, Meng N, Wang J, Liu W, Wang X, Yan M, *et al*. Comparative analysis of the value of diffusion kurtosis imaging and diffusion-weighted imaging in evaluating the histological features of endometrial cancer. Cancer Imaging: the Official Publication of the International Cancer Imaging Society. 2019; 19: 9.

[22] Peeken JC, Spraker MB, Knebel C, Dapper H, Pfeiffer D, Devecka M, *et al*. Tumor grading of soft tissue sarcomas using MRI-based radiomics. EBioMedicine. 2019; 48: 332–340.

[23] Abbasian Ardakani A, Bureau NJ, Ciaccio EJ, Acharya UR. Interpretation of radiomics features-A pictorial review. Computer Methods and Programs in Biomedicine. 2022; 215: 106609.

[24] Wu Q, Shi D, Dou S, Shi L, Liu M, Dong L, *et al*. Radiomics Analysis of Multiparametric MRI Evaluates the Pathological Features of Cervical Squamous Cell Carcinoma. Journal of Magnetic Resonance Imaging: JMRI. 2019; 49: 1141–1148.

[25] Huang G, Cui Y, Wang P, Ren J, Wang L, Ma Y, *et al*. Multi-Parametric Magnetic Resonance Imaging-Based Radiomics Analysis of Cervical Cancer for Preoperative Prediction of Lymphovascular Space Invasion. Frontiers in Oncology. 2022; 11: 663370.